Prediction and Control of Transition in Supersonic and Hypersonic Boundary Layers

Mujeeb R. Malik*
High Technology Corporation, Hampton, Virginia

In this paper, the role of compressible linear stability theory in prediction of boundary-layer transition at supersonic and hypersonic speeds is investigated. Computations for sharp cones, using the e^N method with N = 10, show that the first oblique Tollmien-Schlichting mode is responsible for transition at adiabatic wall conditions for freestream Mach numbers up to about 7. For cold walls, the two-dimensional second mode dominates the transition process at lower hypersonic Mach numbers due to the well-known destabilizing effect of cooling on the second mode. It is shown that pressure gradient and suction may be used to stabilize this mode. The results also show that compressible stability theory can also be used to predict transition in supersonic boundary layers over concave walls where Görtler vortices constitute the prime instability mechanism.

I. Introduction

THE existence of instability waves in a boundary layer was first demonstrated by the theoretical work of Tollmien[1] more than half a century ago. These waves, known as Tollmien-Schlichting (T-S) waves, were later experimentally verified by Schubauer and Skramstad,[2] who showed that T-S waves preceeded laminar/turbulent transition at the low disturbance level of their wind tunnel. Since these findings, considerable progress has been made in the field of boundary-layer transition prediction using stability theory. Smith[3] put forward a criterion for transition in two-dimensional boundary layers. According to this criterion, transition will take place when T-S waves in the boundary layer have been amplified by a factor of e^N. By comparison with low-speed experimental transition data, Jaffe, Okamura, and Smith[4] found that the exponent N has a value of about 10 for two-dimensional boundary layers with and without pressure gradient.

Later, for three-dimensional boundary layers on a swept-wing leading edge, Srokowski and Orszag[5] and Hefner and Bushnell[6] found that the exponent N (hereafter referred to as N factor) is in the range of 7–11. The instability mechanism involved in the incompressible flat-plate boundary layer and that in the swept-wing case are not the same. For the swept wing, the instability is due to the inflection point in the crossflow velocity profile, which results in disturbance vortices approximately aligned with the meanflow direction. Contrarily, instability in the incompressible flat-plate boundary layer is a viscous instability and results in disturbance vortices that align normal to the meanflow direction. Another three-dimensional boundary layer that has inflectional instability is that on a flat rotating disk. There, however, additional effects of Coriolis forces and streamline curvature are present. Malik, et al.[7] found that when these effects are properly accounted for in the stability equations, the N factor for the rotating disk case is about 11. Similar conclusions were drawn by Malik and Poll for a swept cylinder.[8] Even in the case of Görtler vortices, which are caused due to centrifugal instability, calculations performed by Smith[9] suggest that the value of N is around 10.

What all this evidence means physically is that the breakdown to turbulence takes place when the disturbance waves in two- or three-dimensional boundary layers approach a range of critical amplitudes, whatever the mechanism of instability might be. When the external disturbances are "sufficiently" small, the amplification of the infinitesimal instability waves prior to transition is evidently the order of e^{10}. In the presence of a more intense external disturbance environment (vorticity, roughness, vibration, acoustic, etc.), however, the allowed amplification between the critical point and the transition onset will be much smaller. Mack[10] correlated the N factor with freestream turbulence for incompressible flat-plate boundary-layer transition data of Dryden[11] and found that N reduces from 8.1 to 2.6 when freestream turbulence intensity is increased from 0.1% to 1%.

In supersonic wind-tunnel experiments, the significance of the freestream turbulence (vorticity) is greatly reduced with increasing Mach numbers due to large accelerations from the settling chamber to the test section. However, the sound field radiated by the turbulent tunnel-wall boundary layers constitutes a unique supersonic stream disturbance source, which is somehow "internalized" in the test model boundary layer and causes early transition. The work of Pate and Schueler[12] clearly showed the adverse effect of radiated noise on the transition Reynolds numbers. Mack[13] put forward a forcing theory to simulate the response of the boundary layer to incoming sound. His results compared favorably with the experiment of Kendall[14] at $M_\infty = 4.5$ in the JPL 20-in. tunnel. In any case, the amplification, calculated by the stability theory, in the postcritical region prior to transition, is very small due to initially large amplitudes present at the critical point because of strong external disturbances in the conventional supersonic wind tunnels. The same is true for hypersonic wind tunnels. The question remains that, if the external disturbances were very weak, will the compressible stability theory predict amplfication of T-S waves of the order of e^{10} at the onset of transition for various flow configurations?

This question has important ramifications for supersonic laminar flow control and the design of the National Aerospace Plane (NASP). For the latter application, in particular, the knowledge of the exact location of transition is crucial for proper aero/thermal design. Currently, no predictive capability exists for transition in hypersonic boundary layers.

In this paper, linear compressible stability theory is used to study the stability of high-speed boundary layers over flat plates and sharp cones. The question of control of boundary layers using cooling, pressure gradient, and suction is considered. We use the e^N method to correlate with existing low-dis-

Received March 31, 1988.

*President, Senior Member AIAA.

turbance transition data at Mach numbers up to 7. Calculations are also presented for Görtler vortices in supersonic boundary layers.

II. Problem Formulation

We consider boundary-layer flow past two-dimensional or axisymmetric bodies. The governing equations for the basic state whose stability is the subject of this paper can be derived using the Mangler-Levy-Lees transformation:

$$d\xi = \rho_e \mu_e u_e (r_0(x)/L_r)^{2j}\, dx$$

$$d\eta = [\rho_e u_e/(2\xi)^{1/2}](r/L_r)^j(\rho/\rho_e)\, dy$$

where ρ_e is the edge density, μ_e the viscosity, u_e the velocity, r_0 the body radius, L_r a reference length, x the distance along the body and y normal to it. The exponent $j=0$ for a two-dimensional body, and $j=1$ for axisymmetric body. In $\xi-\eta$ coordinates, the governing equations for the boundary-layer flow may be written as

$$(cf'')' + ff'' + \bar{\beta}[\rho_e/\rho - (f')^2] = 2(f'\frac{\partial f'}{\partial \xi} - f''\frac{\partial f}{\partial \xi}\xi) \qquad (1)$$

$$(a_1 g' + a_2 f' f'')' + fg' = 2\xi(f'\frac{\partial g}{\partial \xi} - g'\frac{\partial f}{\partial \xi} \qquad (2)$$

where

$$f' \equiv u/u_e, \quad c \equiv (1+\chi)^{2j}\rho\mu/\rho_e\mu_e, \quad \bar{\beta} \equiv (2\xi/u_e)(du_e/d\xi)$$

$$g \equiv H/H_e, \quad a_1 = c/Pr, \quad a_2 \equiv c\frac{u_e^2}{H_e}(1 - \frac{1}{Pr})$$

and χ is the transverse curvature parameter, $\bar{\beta}$ the pressure gradient parameter, Pr the Prandtl number, and H the enthalpy. In the present study, the dynamic viscosity is prescribed by the Sutherland's law.

We consider harmonic disturbances of the form

$$\tilde{\phi}(x,y,z,t) = \hat{\phi}(y)e^{i(\alpha x + \beta z - \omega t)}$$

imposed upon the basic flow where ϕ represents disturbance flow variables such as velocity, temperature, pressure, etc. Here, ω is the disturbance frequency, α the wavenumber along the body, and β the wavenumber in the azimuthal direction. The resulting flow (mean + perturbation) is substituted into the compressible Navier-Stokes equations represented in body-fitted coordinate system. The equations are then linearized and an eigenvalue problem for α, β, and ω is obtained. For temporal stability, α, β are real, and ω is complex, while, for spatial stability, the converse is true. The governing equations may be represented as

$$A\frac{d^2\hat{\phi}}{dy^2} + B\frac{d\hat{\phi}}{dy} + C\hat{\phi} = 0 \qquad (3)$$

with homogeneous boundary conditions on $\hat{\phi} \equiv [\hat{u}, \hat{v}, \hat{p}, \hat{T}, \hat{w}]^T$.

Here

$$A = \begin{bmatrix} 1 & & & & \\ & 1 & & \bigcirc & \\ & & 0 & & \\ & \bigcirc & & 1 & \\ & & & & 1 \end{bmatrix}$$

and B and C are 5×5 matrices dependent upon the mean flow and disturbance characteristics. These have been given by Malik[15] in Cartesian coordinates. The coefficients in body-oriented coordinates are given elsewhere.[16]

Equation (3) may also be represented as a system of first-order equations:

$$\frac{d\Omega_i}{dy} - \sum_{j=1}^{8} a_{ij}\Omega_j = 0; \qquad i = 1,2,\ldots,8 \qquad (4)$$

where

$$\Omega_1 = \hat{u} \qquad (5a)$$

$$\Omega_2 = \frac{d\hat{u}}{dy} \qquad (5b)$$

$$\Omega_3 = \hat{v} \qquad (5c)$$

$$\Omega_4 = \hat{p} \qquad (5d)$$

$$\Omega_5 = \hat{T} \qquad (5e)$$

$$\Omega_6 = \frac{d\hat{T}}{dy} \qquad (5f)$$

$$\Omega_7 = \hat{w} \qquad (5g)$$

$$\Omega_8 = \frac{d\hat{w}}{dy} \qquad (5h)$$

and a_{ij} is an 8×8 matrix. The coefficients a_{ij} have been given by Mack[17] in Cartesian coordinates.

For a two-dimensional disturbance ($\psi = \tan^{-1}(\beta/\alpha) = 0$), the governing equations reduce to a sixth-order system since the azimuthal disturbance $\hat{w}$ is then identically zero.

There are several numerical methods available for the solution of compressible linear eigenvalue problem. Here we use the finite-difference matrix method of Malik[18] for Eq. (3) and the fourth-order compact difference scheme of Malik, Chuang, and Hussaini[19] for Eq. (4). The latter method is particularly suited for hypersonic boundary-layer stability since it allows fourth-order accuracy on arbitrarily distributed grids. The critical layer in hypersonic boundary layers is located near the edge of the boundary layer and the two-point compact difference scheme allows it to be properly resolved. For the first (three-dimensional) mode, we have employed group velocity transformations to convert the temporal growth rate of the method of Ref. 18 to the spatial growth rate. The second mode computations were made using spatial stability with the method of Ref. 19.

In e^N method, the exponent N may be defined as

$$N = \ln(A/A_0) = -\int_{x_0}^{x} \alpha_i\, dx \qquad (6)$$

where $-\alpha_i$ is the growth rate of the disturbance, x_0 the location of onset of instability, and A_0 the disturbance amplitude there. For transition correlation purposes, Eq. (6) is solved for various disturbance frequencies, and the frequency that most amplifies up to the transition onset location x_{tr} provides the relevant N factor. Consistent with previous findings[4-9,20] we choose $N=10$ for transition prediction. This value gives the location of initiation of transition and not the end of it.

III. Results and Discussion

Compressible Boundary-Layer Stability and Effect of Cooling

Some of the early work on compressible stability theory for flat plate boundary layers was done by Lees and Lin,[21] Lees and Reshotko,[22] and Mack.[23] An excellent review on the subject has been provided by Mack.[17] It has been found that the instability in a compressible boundary layer is both of viscous and inviscid nature. A sufficient condition for the existence of an amplified inviscid disturbance is the presence of a generalized inflection point $[(d/dy)(\rho du/dy) = 0]$ at some $y > y_0$, where y_0 is the point where $U = 1 - 1/M_e$. An insulated compressible flat-plate boundary layer always has this inflection point, and thus, is subjected to inviscid disturbances. At low Mach numbers the instability is of the viscous type (meaning that the maximum amplification rate increases as the Reynolds number is decreased) just as in incompressible flow with a significant difference that the most amplified disturbances are oblique, and Squire's theorem no longer holds true. This oblique mode is referred to as the first T-S mode. As the Mach number increases, the generalized inflection point moves outwards in the boundary layer, and the nature of the first mode changes from the viscous to inviscid type just as in an incompressible boundary layer with adverse pressure gradient, though compressibility has a stabilizing effect. Above about $M_e = 4$, the influence of viscosity is only stabilizing on the first mode disturbances. As the boundary layer is cooled, a second generalized inflection point appears for $U < 1 - 1/M_e$. With increased cooling, the second generalized inflection point moves outwards and finally they both disappear. When this happens, the first mode inviscid disturbances are stabilized. However, as the Mach number increases the amount of cooling required to stabilize the first mode also increases.

Mack,[23] by numerical computations, showed that in addition to the disturbance mode mentioned above, there exists an infinite sequence of discrete modes if $\overline{M}^2 > 1$ somewhere in the boundary layer where

$$\overline{M}^2 = (\alpha U - \omega) M_e / [(\alpha^2 + \beta^2) T]^{1/2} \tag{7}$$

These modes, referred to as higher modes, do not require the presence of a generalized inflection point and only the above condition of $\overline{M}^2 > 1$ is sufficient for inviscid disturbances to exist. This condition is first satisfied at $M_e = 2.2$ in an insulated flat-plate boundary layer and this is also the lowest Mach number where neutral subsonic higher mode disturbances can exist. The first of these modes is commonly referred to as the second mode. This is also known to be the most amplified of the higher modes.

The lowest Mach number at which the unstable second mode region has been located at finite Reynolds numbers is $M_e = 3$, where the minimum critical Reynolds number $R = \sqrt{Re_x}$ is 13,900.[17] As the Mach number increases, the critical Reynolds number for second mode rapidly decreases. At Mach 4.5, it is only 235.[17] Contrary to the first T-S mode, the second mode is, in general, more unstable when $\psi = 0$. The significance of the second mode to hypersonic boundary-layer transition is brought out by the fact that it has much hig' er growth rates than the first oblique mode. More signific' ly, the second mode cannot be stabilized by cooling. In fact i is destabilized since the region in the boundary layer where $\overline{M}^2 > 1$ is satisfied expands with cooling.

Calculations have been performed to study the effect of cooling on both the first and second modes. The results are presented in Fig. 1. The first mode calculations for $M_e = 2$ and 4.5 are made by assuming $\psi = 60$ deg, $R = 1500$ and a stagnation temperature of 560°R. The growth rate for Mach 2 flow decreases rapidly with cooling and $\psi = 60$ deg disturbance is completely stabilized when $T_w/T_{adb} = 0.7$. However, for $M_e = 4.5$ the oblique wave is stabilized only when $T_w/T_{adb} \simeq 0.48$. The second mode on the other hand is destabilized by cooling as shown in Fig. 1. The growth rate for the most amplified disturbance increases quite rapidly with cooling.

The frequency of the most amplified first mode disturbance decreases with wall cooling. We define the nondimensional frequency as $F = 2\pi h\, \nu_e / U_e^2$ where h is the frequency in hertz and V_e is the kinematic viscosity. For $M_e = 2$, the frequency decreased from $F = 0.12 \times 10^{-4}$ to $F = 0.1 \times 10^{-4}$ when T_w/T_{adb} is varied from 1 to 0.7, while for $M_e = 4.5$, F changed from 0.24×10^{-4} to 0.12×10^{-4} when T_w/T_{adb} drops to 0.5. Contrarily, the frequency of the most amplified second mode disturbance increases with wall cooling as depicted in Fig. 2 where the unstable frequency band shifts to the higher frequencies with much larger peak amplification rates. In other words, a fixed second-mode frequency is stabilized with sufficient cooling, but the most amplified disturbance belongs to higher and higher frequencies. The destabilizing effect of cooling on the second mode continues to be present at higher Mach numbers. An example is provided in Fig. 3, where calculations are made for $M_e = 10$, $F = 0.9 \times 10^{-4}$ and $T_e = 480$ R. The wall temperature is assumed to be 2000 R and 1000 R. The same effect of cooling as in Mach 4.5 flow is found here. The sensitivity to changes in wall temperature decreases, however, with Mach number. The shift of the most amplified disturbances to the higher frequencies may be suggesting that if the "environment" were free of high-frequency disturbances, cooling may actually stabilize a hypersonic boundary layer.

Second Mode Control with Pressure Gradient and Suction

It has already been shown that cooling cannot be used to stabilize the second mode. Since laminar flow control may be beneficial for hypersonic flight, the question is as follows: Can

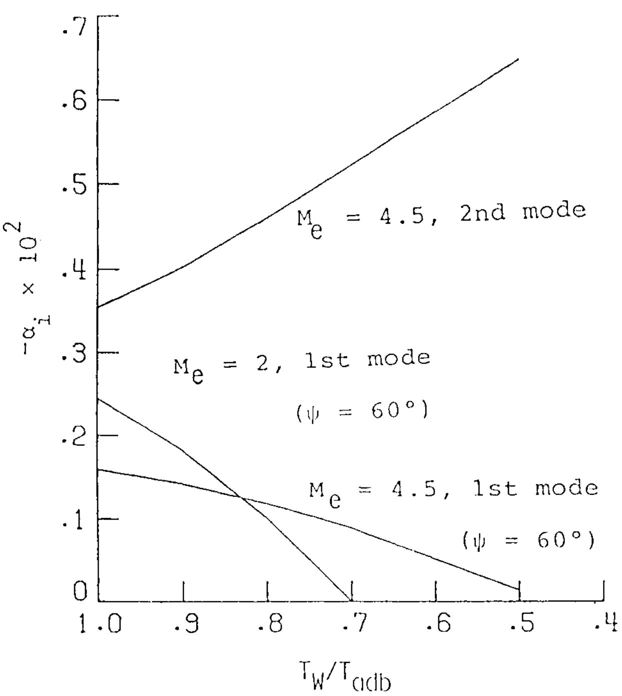

Fig. 1 Effect of wall cooling on the amplified first and second mode disturbances in a flat-plate boundary layer at $R = 1500$.

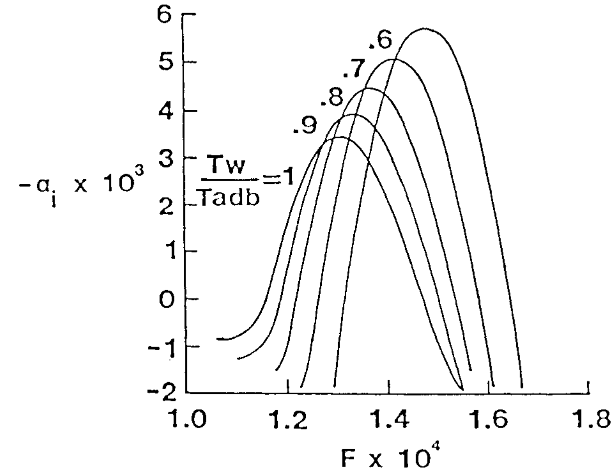

Fig. 2 Effect of wall cooling on second-mode instability in Mach 4.5 boundary layer at $R = 1500$.

the second mode be controlled? Heating is an obvious answer, but, as a practical matter, it may have limited use, since high wall temperatures may not be sustained by the available materials. Furthermore, first T-S mode is destabilized by wall heating.

Wall suction and favorable pressure gradient (wall shaping) have an effect on the generalized inflection point similar to that of cooling. So, the first oblique mode can be stabilized by suction and favorable pressure gradients. The second mode, however, is not dependent upon the presence of a generalized inflection point. For its existence, a region in the boundary layer must be present where $\overline{M}^2 > 1$ [see Eq. (7)] according to the inviscid theory. Here, we use viscous theory to study the effect of pressure gradient and suction on the second mode instability.

We have made computations for $M_e = 4.5$, $R = 1500$, and various values of the pressure gradient parameter $\overline{\beta}$. The positive values of this parameter pertain to favorable gradients. The results are presented in Fig. 4. The band of unstable disturbances moves very quickly to higher nondimensional frequencies just as in Fig. 2 due to cooling. However, the peak amplification rate now decreases, and there is no instability at this Reynolds number for $\overline{\beta} \geq 0.075$. One objection could be raised about these computations. Mean flow was computed by setting the right-hand sides of Eqs. (1) and (2) to zero. For nonzero $\overline{\beta}$, a_2 in Eq. (2) would vary with ξ, and similarity can be strictly assumed only for a Prandtl number of unity. In the present computations, the Prandtl number varied and was close to 0.7. Calculations were also made for a nonsimilar boundary layer that developed on the wall of a hypersonic nozzle with a suction slot ahead of the throat.[24] The flow accelerated from Mach 0.34 at the lip of the suction slot to Mach 6 towards the exit of the nozzle. The pressure gradient was higher in the early part of the nozzle, and it steadily decreased as the exit was approached. For computations, we chose a station along the wall where $M_e = 4.57$ to approximate the Mach number in Fig. 4. The local stability Reynolds number is, however, almost twice ($R = 3165$) and local value of $\overline{\beta} = 0.186$. The results show no trace of instability as shown in Fig. 5. For reference, zero pressure gradient ($\overline{\beta} = 0$) results at the local conditions of Reynolds number and Mach number are also presented in the figure. Calculations were also performed at another nozzle station where $M_e = 5.45$, $R = 3648$ and $\overline{\beta} = 0.098$. The results are presented in Fig. 6. The second-mode instability is now present, but the peak growth rate is much less than the zero pressure gradient case with the same value of M_e and R.

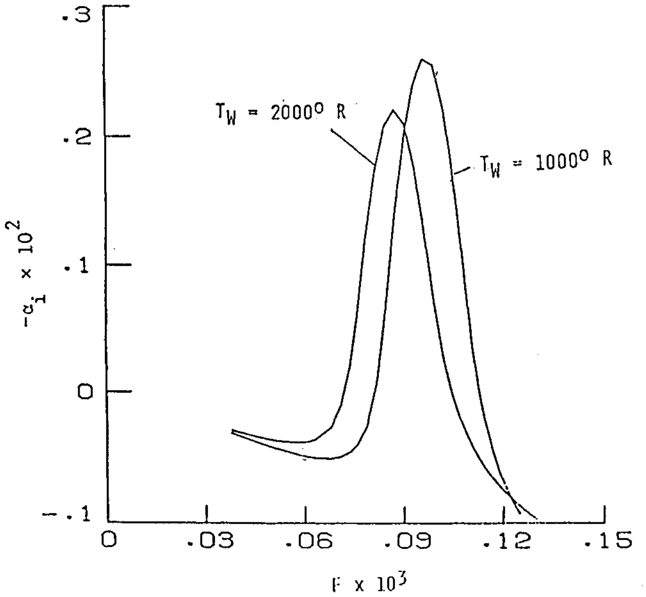

Fig. 3 Effect of wall temperature on second-mode instability in Mach 10 boundary layer at $R = 1000$.

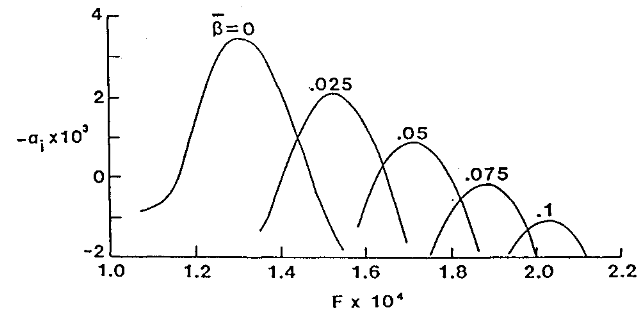

Fig. 4 Effect of pressure gradient on the second-mode instability in a boundary layer at $M_e = 4.5$ and $R = 1500$.

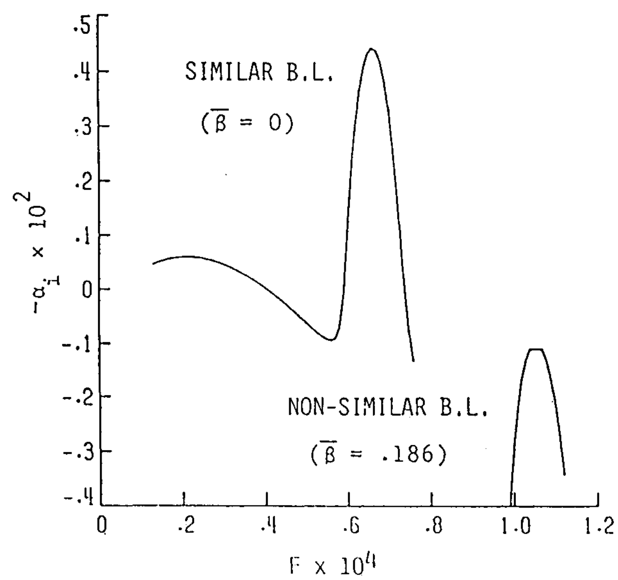

Fig. 5 Effect of pressure gradient on the second-mode instability in a boundary layer at $M_e = 4.57$ and $R = 3165$.

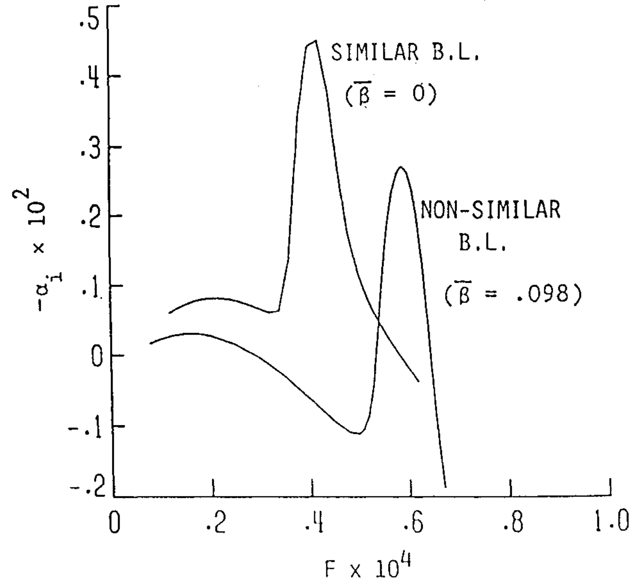

Fig. 6 Effect of pressure gradient on the second-mode instability in a boundary layer at $M_e = 5.45$ and $R = 3648$.

The effect of suction was considered next. Calculations were made for $M_e = 4.5$ and $R = 1500$. Disturbance growth rate results for various values of the suction parameter are presented in Fig. 7. The effect of suction on the disturbance frequency is the same as with favorable pressure gradient. Complete stabilization at this Reynolds number is achieved for the suction parameter value $f_w = 0.4$. Here $f_w = -\sqrt{2}\ R\ \rho_w v_w/\rho_e u_e$. The value of $f_w = 0.4$, therefore, corresponds to $\rho_w v_w/\rho_e u_e = -1.88 \times 10^{-4}$. This will be expected to increase with Mach number.

Transition Prediction

Historically, conventional supersonic wind tunnels produce very low transition Reynolds numbers, which then result in low N factors. The applicability of e^N method to supersonic flows, therefore, has been questioned. We have pointed out, however, that e^N method by its very nature is applicable only when the freestream disturbance environment is not strong enough to dictate the transition process in the boundary layer. In conventional wind tunnels, this is certainly not the case, and it is futile to think that e^N will be a predictor of transition in those tunnels and other highly disturbed environments. Transition, for its prediction, in such situations would require a complete qualitative and quantitative knowledge of the environment before one can even begin to ponder into the complex problem of "receptivity." The ability to obtain this knowledge is a problem in its own right. Advances, however, can be made in correlating and predicting transition in "similarly disturbed environments."

When transition takes place in a low-disturbance environment, a properly employed e^N method provides a useful tool for transition prediction even in supersonic flow.[20] Flight transition data have been compiled for sharp cones by Beckwith[25] for various Mach numbers and are shown in Fig. 8. The figure also contains a correlation for wind-tunnel transition data given by Beckwith, which lies much below the flight data. The flight data are for varying conditions of wall temperatures whose distribution is not known in many cases. A direct comparison with the data, therefore, cannot be made. We have made calculations for 5 deg (half-angle) cones for various Mach numbers up to 7. The wall was assumed to be adiabatic, and transition was said to occur when $N = 10$ is first reached by an unstable frequency. The predicted variation of transition Reynolds number with Mach number is also plotted in Fig. 8. The predicted curve is in reasonable agreement with some of the flight data and the adiabatic wall data of Fisher and Dougherty[26] and Beckwith, et al.[27] in particular. The latter data were taken in the Langley low-disturbance Mach 3.5 quiet wind tunnel. However, a lot of data lies above the predicted curve for $M_e < 4.5$ and all the data lie below this curve at $M_e \simeq 6$. This is due to the differing effect of cooling on the first- and second-mode disturbances. A calculation was made where the dependence of the wall temperature with Mach number was assumed to be

$$T_w/T_{adb} = 1 - 0.05M_\infty - 0.0025M_\infty^2 \tag{8}$$

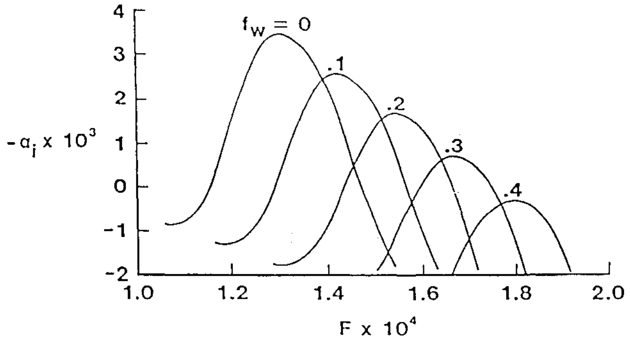

Fig. 7 Effect of wall suction on the second-mode instability in a boundary layer at $M_e = 4.5$ and $R = 1500$.

Equation (8) has no basis except that it was considered reasonable to assume that the ratio T_w/T_{adb} should decrease with Mach number. This ratio was 0.89 at $M_\infty = 2$ and 0.53 at $M_\infty = 7$. Now the predicted transition Reynolds number is much higher for $M_e < 4.5$ in agreement with some of the flight data, and, due to destabilization of the second mode, the predicted transition Reynolds number falls below the adiabatic value of $M_e > 5.5$. The predictions therefore are in general agreement with the flight transition data.

The predictions at $M_\infty = 5$ ($M_e = 4.7$), 6 ($M_e = 5.6$) and 7 ($M_e = 6.4$) require special consideration. Results for these three cases are presented in Figs. 9–11. Figure 9 contains four curves of N vs R for the most amplified frequencies at $N = 10$. Two of the curves belong to first-mode frequencies with and without cooling while the other two curves are for second-mode frequencies. At this Mach number, the first mode is much more amplified than the second mode at adiabatic wall conditions. The second-mode N factor is only 5 at the location where transition is predicted by the first mode using $N = 10$. This is despite the fact that second-mode growth rates are much higher; however, their extent in x is much shorter. When the wall is cooled, the first mode becomes more stable, while the second mode is more unstable. The extent over which a given second-mode frequency is unstable increases, thus reaching $N = 10$ prior to the first mode. The role of the first and second mode is therefore switched.

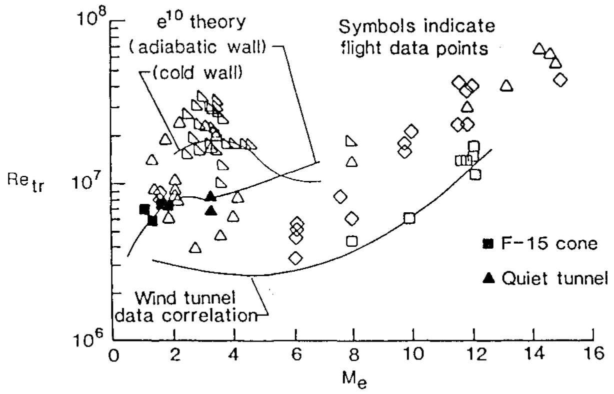

Fig. 8 Comparison of predicted and observed transition Reynolds numbers on sharp cones.

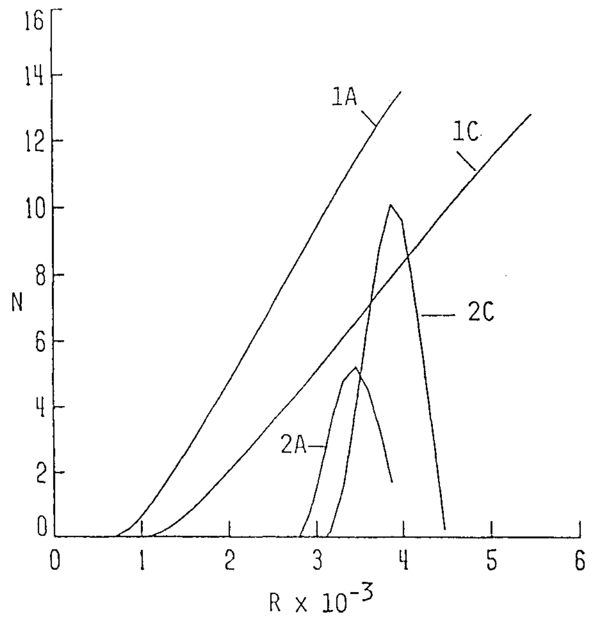

Fig. 9 Computed variation of N with Reynolds number on a 5 deg (half-angle) sharp cone in Mach 5 flow for most amplified frequencies (at $N = 10$): 1A—First mode, adiabatic wall; 1C—First mode, cold wall; 2A—Second mode, adiabatic wall; 2C—Second mode, cold wall.

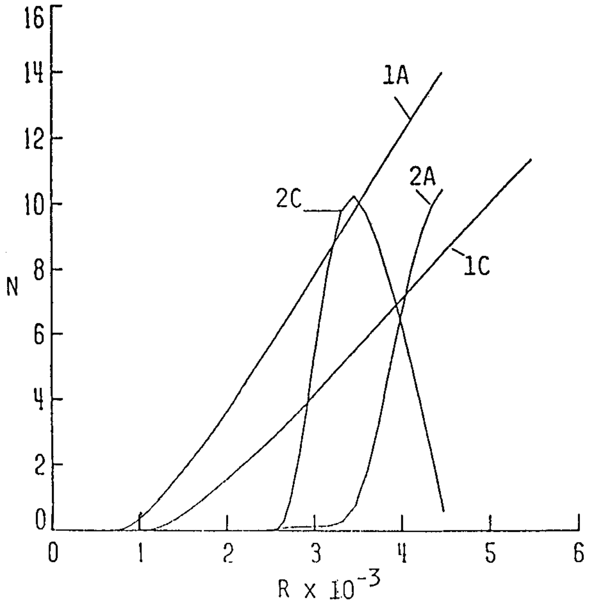

Fig. 10 Same as Fig. 9 except for Mach 6 flow.

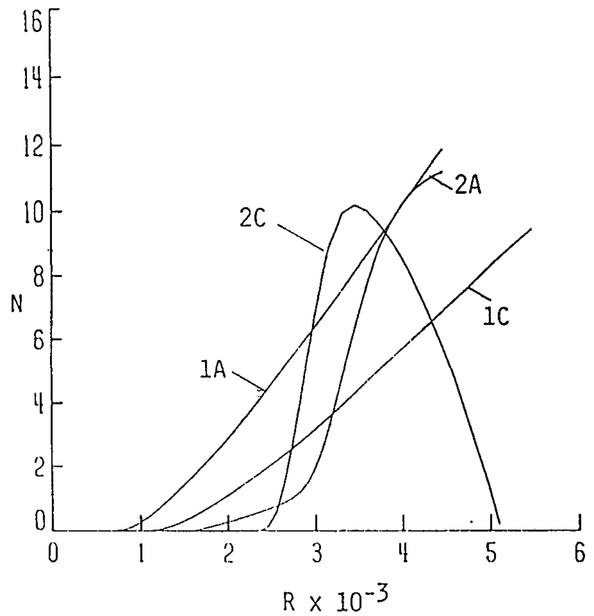

Fig. 11 Same as Fig. 9 except for Mach 7 flow.

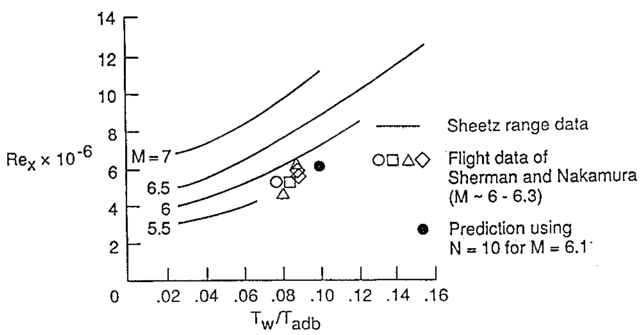

Fig. 12 Comparison with sharp cone transition data in flight and in the range.

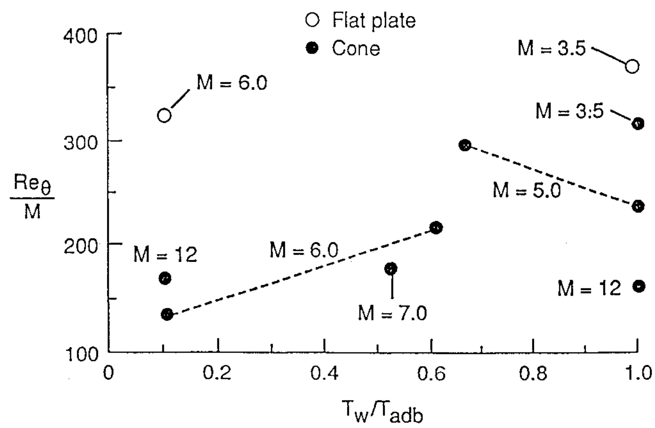

Fig. 13 Value of Re_θ/M at predicted location of transition using $N = 10$ and Mach number M evaluated at the edge of the boundary layer.

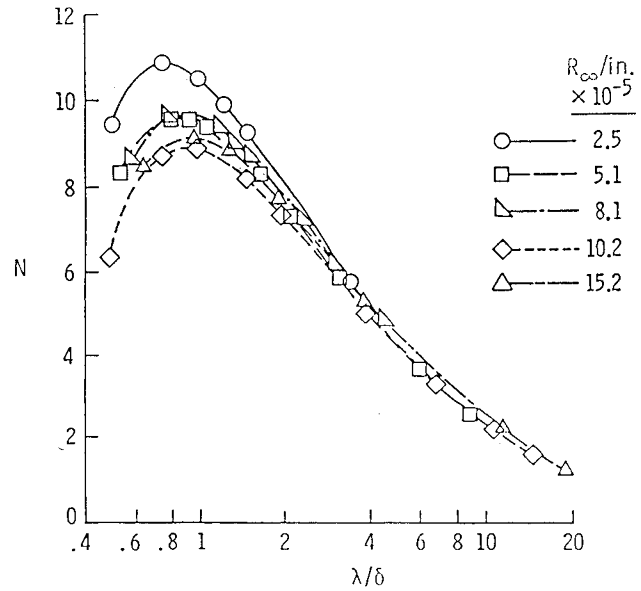

Fig. 14 Effect of Görtler vortex wavelength on integrated amplification to transition in the quiet tunnel nozzle wall.

Results similar to Fig. 9 are presented in Fig. 10 for $M_\infty = 6$. At adiabatic wall conditions the first mode still is dominant and causes transition. When cooled, the second mode is the cause for transition. It should be noted that the curves in Figs. 9-11 are not the envelope curves and actually represent most amplified frequencies. These frequencies are given in Table 1. Figure 11 contains the results for $M_\infty = 7$. It is at this Mach number that both modes amplify to $N = 10$ at the same Reynolds number for adiabatic wall conditions. The second mode calculations were performed by assuming $\psi = 0$. If oblique disturbances were allowed in this calculation, the second mode frequency would yield somewhat higher N factor. It

Table 1 Most amplified frequencies and predicted transition Reynolds numbers for 5 deg (half-angle) sharp cones and boundary layer edge temperature of 200° R.

M_∞	Frequency and transition Reynolds number	Adiabatic wall 1st Mode	Adiabatic wall 2nd Mode	Cold wall [Eq. (8)] 1st Mode	Cold wall [Eq. (8)] 2nd Mode
5	$F \times 10^4$	0.3	–	0.15	1.075
	$Re_{tr} \times 10^{-6}$	10	–	20	15
6	$F \times 10^4$	0.25	0.7	0.15	0.98
	$Re_{tr} \times 10^{-6}$	12	19	25	11.5
7	$F \times 10^4$	0.25	0.65	0.15	0.835
	$Re_{tr} \times 10^{-6}$	16	16	>30	11.2

appears then, that for adiabatic conditions, transition in a 5 deg half-angle sharp-cone boundary-layer will be dominated by second-mode disturbances only when M_∞ approaches a value of about 7 or slightly less. This appears to be consistent with the observations of Kendall.[14] The actual value of M_∞ where the switch takes place will be a function of cone angle, free-stream temperature and wall temperature.

We have also made e^{10} calculations for a sharp cone at $M_e = 6.1$ and $T_w/T_{adb} = 0.1$. The predicted transition Reynolds number is presented in Fig. 12 where the range data of Sheetz[28] and the flight data of Sherman and Nakamura[29] are also plotted as a function of wall temperature. Our calculation is in general agreement with both of the experimental transition data. Comparison with Fig. 8 also shows the severe effect cooling has on the second mode instability.

Designers in the aerospace industry are familiar with a transition correlation that uses the ratio Re_θ/M as the predictor of transition. This correlation is based upon some high Mach number experimental data for cones and, according to it, transition occurs when $Re_\theta \approx 150$. We have performed e^{10} calculation for sharp cones and flat plates at various Mach number and wall temperatures. The results are presented in Fig. 13. The Mach 12 calculations are for helium, which was considered a perfect gas with $\gamma = 1.6667$ and a power law distribution of viscosity. It can be seen that the value of Re_θ/M varies considerably and is vastly different for a flat plate and a sharp cone. Such a correlation, therefore, has very limited use.

So far, we have only considered Tollmien-Schilchting instability. However, e^{10} method may also be used for other instability mechanisms including Görtler vortices in supersonic boundary layers. We used compressible stability theory to perform such a calculation. Calculations were made for a Mach 3.5 nozzle wall for which location of transition was known.[30] Transition occurred in the region of concave curvature and linear stability calculation showed that Tollmien-Schlichting instability was absent due to strong favorable pressure gradient. Calculations for Görtler instability were performed using the method of reference.[19] The results are presented in Fig. 14. Calculations were performed from the start of instability to the observed transition location for various vortex wavelengths for five different unit Reynolds numbers. More details about the test condition are given in Ref. 30. The values of N as a function of vortex wavelength scaled with boundary-layer thickness at transition location are plotted in the figure. The maximum value of N lies in the range of 9–11 for all test conditions, indicating that e^{10} method is a good correlation for transition even when Görtler vortices cause transition in supersonic boundary layers.

Conclusions

Compressible linear stability of supersonic and hypersonic boundary layers on plates and sharp cones at zero angle of attack has been studied. It is shown that, in a low-disturbance environment, the e^N method (with $N = 10$) provides a reliable prediction of transition in supersonic and hypersonic boundary layers on cones and plates. It is also shown that, for adiabatic wall conditions, the first oblique mode is mainly responsible for transition on sharp cones at Mach numbers up to about 7. For cold walls, the role of the second mode becomes increasingly important at much lower Mach numbers due to the well-known destabilizing effect of cooling. Numerical computations using viscous theory show that the second mode can be stabilized with suction and favorable pressure gradients.

Acknowledgment

The support provided by NASA Contract NAS1-18240 is appreciated.

References

1 Tollmien, W., "Uber die Entstehung der Turbulenz," Nachr. Ges. Wiss. Göttingen, Math.-Phys. Klasse, 1929, pp. 21–44.

2 Schubauer, G. B. and Skramstad, H. K., "Laminar Boundary Layer Oscillations and Transition on a Flat Plat," *J. Aero. Sci.*, Vol. 14, 1947, pp. 69–78.

3 Smith, A.M.O., "Transition, Pressure Gradient and Stability Theory," IX International Congress for Applied Mechanics, Brussels, 1956.

4 Jaffe, N. A., Okamura, T.T., and Smith, A.M.O., "Determination of Spatial Amplification Factors and Their Application to Predicting Transition," *AIAA Journal*, Vol. 8, Feb. 1970, pp. 301–308.

5 Srokowski, A. J. and Orszag, S. A., "Mass Flow Requirements for LFC Wing Design," AIAA Paper 77-1222, Aug. 1977.

6 Hefner, J. N. and Bushnell, D. M., "Application of Stability Theory to Laminar Flow Control," AIAA Paper 79-1493, July 1979.

7 Malik, M. R., Wilkinson, S. P., and Orszag, S. A., "Instability and Transition in Rotating Disk Flow," *AIAA Journal*, Vol. 19, Sept. 1981, pp. 1131–1138.

8 Malik, M. R. and Poll, D. I. A., "Effect of Curvature on Three-Dimensional Boundary-Layer Stability," *AIAA Journal*, Vol. 23, Sept. 1985, pp. 1362–1369.

9 Smith, A.M.O., "On the Growth of Taylor-Görtler Vortices Along Highly Concave Walls," *Quarterly Applied Mathematics*, Vol. 13, Oct. 1955, pp. 233–262.

10 Mack, L. M., "Transition Prediction and Linear Stability Theory," AGARD CP-224, May 1977.

11 Dryden, H. L., "Transition from Laminar to Turbulent Flow," *Turbulent Flows and Heat Transfer*, edited by C. C. Lin, Princeton University Press, Princeton, NJ, 1959, pp. 1–74.

12 Pate, S. R. and Schueler, C. J., "Radiated Aerodynamic Noise Effects on Boundary Layer Transition in Supersonic and Hypersonic Wind Tunnels," *AIAA Journal*, Vol. 7, March 1969, pp. 450–457.

13 Mack, L. M., "Linear Stability Theory and the Problem of Supersonic Boundary Layer Transition," *AIAA Journal*, Vol. 13, March 1975, pp. 278-289.

14 Kendall, J. M., "Wind Tunnel Experiments Relating to Supersonic and Hypersonic Boundary Layer Transition," *AIAA Journal*, Vol. 13, March 1975, pp. 290–299.

15 Malik, M. R., "Finite-Difference Solution of the Compressible Linear Eigenvalue Problem," NASA CR-3584, June 1982.

16 Malik, M. R., "Stability for a Sharp Cone and Flat Plate Boundary Layer at Supersonic Mach Numbers," American Society of Mechanical Engineers, New York, Feb. 1984, pp. 139–147.

17 Mack, L. M., "Boundary-Layer Linear Stability Theory," AGARD Rept. No. 709, March 1984.

18 Malik, M. R. "COSAL—A Black Box Compressible Stability Analysis Code for Transition Prediction in Three-Dimensional Boundary Layers," NASA CR-165925, May 1982.

19 Malik, M. R., Chuang, S., and Hussaini, M. Y., "Accurate Solution of Compressible Linear Stability Equations," Zeitschrift Für Angewandte Mathematik und Physik, Vol. 33, 1982, March p. 189.

20 Malik, M. R., "Instability and Transition in Supersonic Boundary Layers," *Laminar-Turbulent Boundary Layers*, edited by E. M. Uram and H. E. Weber, Transition in Hypersonic Boundary.

21 Lees, L. and Lin, C. C., "Investigation of the Stability of the Laminar Boundary Layer in a Compressible Fluid," NACA TN 1115, Sept. 1946.

22 Lees, L. and Reshotko, E., "Stability of the Compressible Laminar Boundary Layer," *Journal of Fluid Mechanics*, Vol. 12, April 1962, pp. 555–590.

23 Mack, L. M., "Boundary-Layer Stability Theory," Jet Propulsion Laboratory, Pasadena, CA, Document No. 900-277, Rev. A., Nov. 1969.

24 Beckwith, I. E., Chen, F.-J., and Malik, M. R., "Design and Fabrication Requirements for Low-Noise Supersonic/Hypersonic Wind Tunnels," AIAA Paper 88-0143, Jan. 1988.

25 Beckwith, I. E., "Development of a High Reynolds Number Quiet Tunnel for Transition Research," *AIAA Journal*, Vol. 13, March 1975, pp. 300–306.

26 Fisher, D. F. and Dougherty, N. S., "In-Flight Transition Measurement on a 10° cone at Mach numbers from 0.5 to 2.0," NASA TP-1971, 1982.

27 Beckwith, I. E., Creel, T. R., Chen, F., and Kendall, J. M., "Free Stream Noise and Transition Measurements in a Mach 3.5 Quiet Tunnel," AIAA Paper 83-0042, Sept. 1983.

28 Sheetz, N. W., "Free-flight Boundary Layer Transition Investigations at Hypersonic Speeds," AIAA Paper 65-127, Jan. 1965.

29 Sherman, M. M. and Nakamura, T., "Flight Test Measurements of Boundary-Layer Transition on a Nonablating 22° Cone," *Journal of Spacecraft and Rockets*, Vol. 7, Feb. 1970, pp. 137–142.

30 Beckwith, I. E., Malik, M. R., and Chen, F. J., "Nozzle Optimization Study for Quiet Supersonic Wind Tunnels," AIAA Paper 84-1628, June 1984.